DESY 09-157
ITEP-LAT-2009-13
Edinburgh 2009/12
LTH 844

Probing the finite temperature phase transition with $N_f = 2$ nonperturbatively improved Wilson fermions

V.G. Bornyakov,[1,2] R. Horsley,[3] S.M. Morozov,[2] Y. Nakamura,[4,5]
M.I. Polikarpov,[2] P.E.L. Rakow,[6] G. Schierholz,[7] and T. Suzuki[8,5]

[1] *Institute for High Energy Physics IHEP,*
142281 Protvino, Russia

[2] *Institute of Theoretical and Experimental Physics ITEP,*
117259 Moscow, Russia

[3] *School of Physics and Astronomy,*
University of Edinburgh,
Edinburgh EH9 3JZ, UK

[4] *Institut für Theoretische Physik,*
Universität Regensburg,
93040 Regensburg, Germany

[5] *RIKEN, Radiation Laboratory,*
Wako 351-0158, Japan

[6] *Theoretical Physics Division,*
Department of Mathematical Sciences,
University of Liverpool,
Liverpool L69 3BX, UK

[7] *Deutsches Elektronen-Synchrotron DESY,*
22603 Hamburg, Germany

[8] *Institute for Theoretical Physics,*
Kanazawa University,
Kanazawa 920-1192, Japan

QCDSF–DIK Collaboration

Abstract

The critical temperature and the nature of the QCD finite temperature phase transition are determined for $N_f = 2$ dynamical flavors of nonperturbatively improved Wilson fermions. The calculations are performed on large lattices with temporal extents $N_t = 12$, 10 and 8, and lattice spacings down to $a = 0.075\,\mathrm{fm}$. We find the deconfinement and chiral phase transitions to take place at the same temperature. Our results are in broad agreement with a second order phase transition in the chiral limit. The critical temperature at the physical quark mass is found to be $T_c = 174(3)(6)\,\mathrm{MeV}$.

PACS numbers: 11.15.Ha, 12.38.Aw, 12.38.Gc

I. INTRODUCTION

One of the basic questions in finite temperature QCD is: What is the nature of the finite temperature phase transition, and at which temperature does it happen? In spite of enormous computational efforts [1, 2], the answer to this question has remained controversial. The Wuppertal group [2] finds the deconfining transition, which we identify with the peak of the Polyakov-loop susceptibility, and the chiral transition at widely separated temperatures. In contrast, the Brookhaven/Bielefeld collaboration claims both temperatures to coincide. Furthermore, the Brookhaven/Bielefeld collaboration [3] quotes a transition temperature of $T_c = 196(3)\,\mathrm{MeV}$, while the transition temperatures found by the Wuppertal group [4] are $T_c = 170(7)\,\mathrm{MeV}$ for the deconfining transition and $T_c = 146(5)\,\mathrm{MeV}$ for the chiral transition. Both groups use rooted staggered fermions, but with different levels of improvement. The Brookhaven/Bielefeld collaboration uses *asqtad* as well as *p4* fermions, while the Wuppertal group employs twice iterated stout smeared links in the fermion matrix. It has been argued [2] that the discrepancy is largely due to the rather coarse lattices used by the Brookhaven/Bielefeld collaboration. Indeed, inititial calculations of this group were limited to lattices of temporal extent $N_t \leq 6$, corresponding to lattice spacings of $a \gtrsim 0.2\,\mathrm{fm}$, while the Wuppertal group performed simulations on lattices of extent $N_t = 10$, 8 and 6, and attempted a continuum extrapolation. More recently, the Brookhaven/Bielefeld collaboration has extended their calculations to lattices of temporal extent $N_t = 8$ [5] and found that with decreasing lattice spacing T_c shifted by $5 - 7\,\mathrm{MeV}$ towards smaller values.

The connection between deconfining and chiral transition has been the subject of several phenomenological considerations. Naively, one would expect the temperature of the deconfinement transition to lie below that of the chiral transition, if different at all. This turns out to be the case, for example, in the Polyakov-loop extended Nambu–Jona-Lasinio model [6]. More likely is that both transitions occur at the same temperature, as Polyakov loop and chiral condensate mix at finite dynamical quark masses. The consequence would be a simultaneous enhancement of both the chiral and Polyakov-loop susceptibilities along the transition line [7–10].

To clarify the issue, an independent investigation of the nature of the finite temperature phase transition is needed. In this work we shall perform simulations with $N_f = 2$ dynamical

flavors of nonperturbatively $O(a)$ improved Wilson fermions, so-called clover fermions, and plaquette gauge action on lattices of temporal extent $N_t = 12$, 10 and 8. This action has been successfully employed by the ALPHA, UKQCD, QCDSF and CERN/Rome collaborations in calculations at zero temperature, on whose results we can draw. Besides that, clover fermions have an exact flavor symmetry, which we consider a big advantage over staggered fermions, as the nature of the finite temperature phase transition largely depends on the flavor degrees of freedom. A disadvantage though is the lack of chiral symmetry. Preliminary results of our work have been reported in [11].

The paper is organized as follows. In sec. II we present the action, and in sec. III we introduce the order parameters, which are the main focus of the analysis. The lattice data are presented in sec. IV and in the Appendix. In sec. V we recapitulate the equation of state, that is expected to describe the thermodynamic properties of QCD with two dynamical flavors near the critical point. Relations between second derivatives of the partition function are called Maxwell relations. One such relation connects the chiral susceptibility to the derivative of the plaquette with respect to mass, and will be derived in sec. VI. In sec. VII we compute the transition temperature from the Polyakov-loop susceptibility, the chiral susceptibility and the correlator of Polyakov loop and chiral condensate, and fit its dependence on the quark mass to the prediction of the equation of state. Finally, in sec. VIII we conclude.

II. LATTICE SIMULATION

We consider mass-degenerate sea quarks. The fermionic action for each of the two flavors reads

$$\begin{aligned} S_F = a^4 \sum_x \Big\{ & \frac{1}{2a} \sum_\mu \bar\psi(x)\, U_\mu(x)\, [\gamma_\mu - 1]\, \psi(x + a\hat\mu) \\ & - \frac{1}{2a} \sum_\mu \bar\psi(x)\, U_\mu^\dagger(x - a\hat\mu)\, [\gamma_\mu + 1]\, \psi(x - a\hat\mu) \\ & - c_{SW}\, \frac{i}{2a} \sum_{\mu\nu} \bar\psi(x)\, \sigma_{\mu\nu}\, P_{\mu\nu}(x)\, \psi(x) + (m + m_c)\, \bar\psi(x)\, \psi(x) \Big\} \end{aligned} \tag{1}$$

β	c_{SW}	$V = N_s^3\, N_t$	κ_c	r_0/a
5.20	2.0171	$16^3\, 8$	0.136050(17)	5.454(58)
5.20	2.0171	$24^3\, 10$	0.136050(17)	5.454(58)
5.25	1.9603	$16^3\, 8$	0.136273(7)	5.880(26)
5.25	1.9603	$24^3\, 8$	0.136273(7)	5.880(26)
5.25	1.9603	$32^3\, 12$	0.136273(7)	5.880(26)
5.29	1.9192	$24^3\, 12$	0.136440(4)	6.201(25)

TABLE I: Parameters of the simulation.

where $P_{\mu\nu}$ is the clover-leaf form of the lattice field strength tensor,

$$\begin{aligned} P_{\mu\nu}(x) = \frac{1}{4}\Big[& U_\nu(x)\, U_\mu(x+a\hat{\nu})\, U_\nu^\dagger(x+a\hat{\mu})\, U_\mu^\dagger(x) \\ & + U_\nu^\dagger(x-a\hat{\nu})\, U_\mu^\dagger(x-a\hat{\mu}-a\hat{\nu})\, U_\nu(x-a\hat{\mu}-a\hat{\nu})\, U_\mu(x-a\hat{\mu}) \\ & - U_\nu(x)\, U_\mu^\dagger(x-a\hat{\mu}+a\hat{\nu})\, U_\nu^\dagger(x-a\hat{\mu})\, U_\mu(x-a\hat{\mu}) \\ & - U_\nu^\dagger(x-a\hat{\nu})\, U_\mu(x-a\hat{\nu})\, U_\nu(x+a\hat{\mu}-a\hat{\nu})\, U_\mu^\dagger(x)\Big]\,, \end{aligned} \tag{2}$$

and

$$am_c = \frac{1}{2\kappa_c}\,, \quad am = \frac{1}{2\kappa} - \frac{1}{2\kappa_c} \tag{3}$$

κ_c being the critical value of the hopping parameter. The improvement coefficient c_{SW} was determined nonperturbatively [12].

We use the highly optimized HMC algorithm of the QCDSF collaboration [13] for updating the gauge field. Considerable speedups were obtained by applying mass preconditoning à la Hasenbusch [14] and putting the pseudofermion action on multiple time scales [15]. The algorithm runs about three times faster than an equally optimized RHMC algorithm for $N_f = 2 + 1$ dynamical flavors [16], which was one of the reasons for concentrating on $N_f = 2$ flavors first. The couplings, lattice volumes and lattice spacings covered by our simulations are listed in Table I. The scale parameters r_0/a have been taken from the zero temperature runs of the QCDSF collaboration at the corresponding couplings. They refer to the chiral limit $\kappa = \kappa_c$. We also list the critical hopping parameters κ_c, which we adopted from QCDSF as well. (For recent relevant work see [17].) On each lattice we have performed

simulations at up to 13 different κ values placed around the transition line. The exact values are given in Tables III–V in the Appendix. The temperature of our lattices is given by

$$T = \frac{1}{N_t\, a}\,. \tag{4}$$

The gauge field configurations were generated on the BlueGene/L at KEK, the RSCC cluster at RIKEN, the MVS-50k at the Joint Computer Center (Moscow), on the SKIF-Chebyshev at Moscow State University, as well as on the Altix at HLRN.

III. ORDER PARAMETER

Two-flavor QCD is expected to undergo a second order transition at finite temperature in the chiral limit and at very small quark masses. In the chiral limit the order parameter is the subtracted scalar density $\sigma_- = \sigma - \sigma_0$, defined through

$$\sigma = \frac{a^3}{V} \sum_x \bar{\psi}(x)\psi(x) = Z_S^{-1}\sigma_R + \sigma_0\,, \tag{5}$$

where σ_R is the renormalized density, and σ_0 is an additive renormalization constant, which arises from mixing of σ with the vacuum due to lack of chiral symmetry. For heavy quark masses close to the quenched limit, the theory is known to undergo a first order phase transition. In that limit the order parameter is the Polyakov loop

$$L = \frac{1}{N_s^3} \sum_{\vec{x}} \mathrm{Re}\, L(\vec{x})\,,\; L(\vec{x}) = \frac{1}{3}\,\mathrm{Tr} \prod_{x_4=1}^{N_t} U_4(x)\,. \tag{6}$$

In the intermediate mass region we expect the transition to be a crossover. This scenario is sketched in Fig. 1. An 'order parameter', which interpolates between the two limits, is

$$\omega = \frac{1}{\sqrt{1+(am)^2}}\,\sigma_- + \frac{am}{\sqrt{1+(am)^2}}\,L\,. \tag{7}$$

The temperature of the chiral transition is, for general m, identified with the peak position of the chiral susceptibility

$$\chi_\sigma \equiv \langle\sigma^2\rangle_c = \langle\sigma^2\rangle - \langle\sigma\rangle^2\,, \tag{8}$$

while the peak of the Polyakov-loop susceptibility

$$\chi_L \equiv N_s^3\,\langle L^2\rangle_c\,,\; \langle L^2\rangle_c = \left(\langle L^2\rangle - \langle L\rangle^2\right) \tag{9}$$

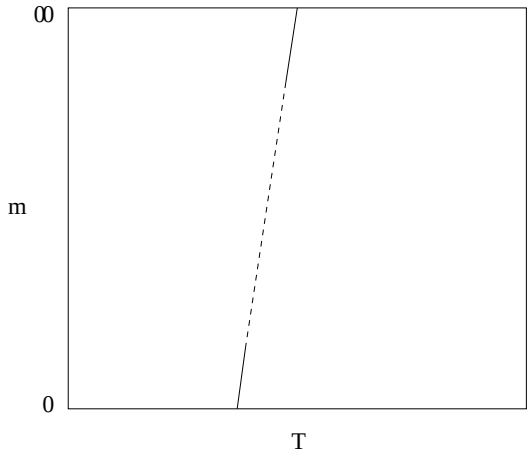

FIG. 1: The phase diagram of two-flavor QCD. The solid lines indicate a second (bottom) and first order transition (top), respectively, while the dashed line denotes the crossover region.

defines the temperature of the deconfining transition. Both, $\langle\sigma^2\rangle_c$ and $\langle L^2\rangle_c$ can be combined into one susceptibility, following (7),

$$\langle\omega^2\rangle_c = \frac{1}{1+(am)^2}\,\langle\sigma^2\rangle_c + \frac{2am}{1+(am)^2}\,\langle L\sigma\rangle_c + \frac{(am)^2}{1+(am)^2}\,\langle L^2\rangle_c\,, \tag{10}$$

where

$$\langle L\sigma\rangle_c = \langle L\sigma\rangle - \langle L\rangle\,\langle\sigma\rangle\,, \tag{11}$$

which interpolates between zero and infinite quark mass. In case the crossover temperature is unique, all three correlators, $\langle L^2\rangle_c$, $\langle L\sigma\rangle_c$ and $\langle\sigma^2\rangle_c$, are expected to peak at the same transition temperature. If, on the other hand, the deconfining and chiral transitions take place at far different temperatures, we would not expect to find a distinct peak in the correlator $\langle L\sigma\rangle_c$. In the connected correlators $\langle\sigma^2\rangle_c$ and $\langle L\sigma\rangle_c$ the additive renormalization constant σ_0 drops out, which allowed us to replace σ_- by σ.

IV. DATA

To compute the chiral susceptibility χ_σ and the correlator of L and σ, $\langle L\sigma\rangle_c$, all we need to know is the average plaquette

$$P = \frac{1}{3}\,\mathrm{Tr}\,\langle U_\Box\rangle\,, \tag{12}$$

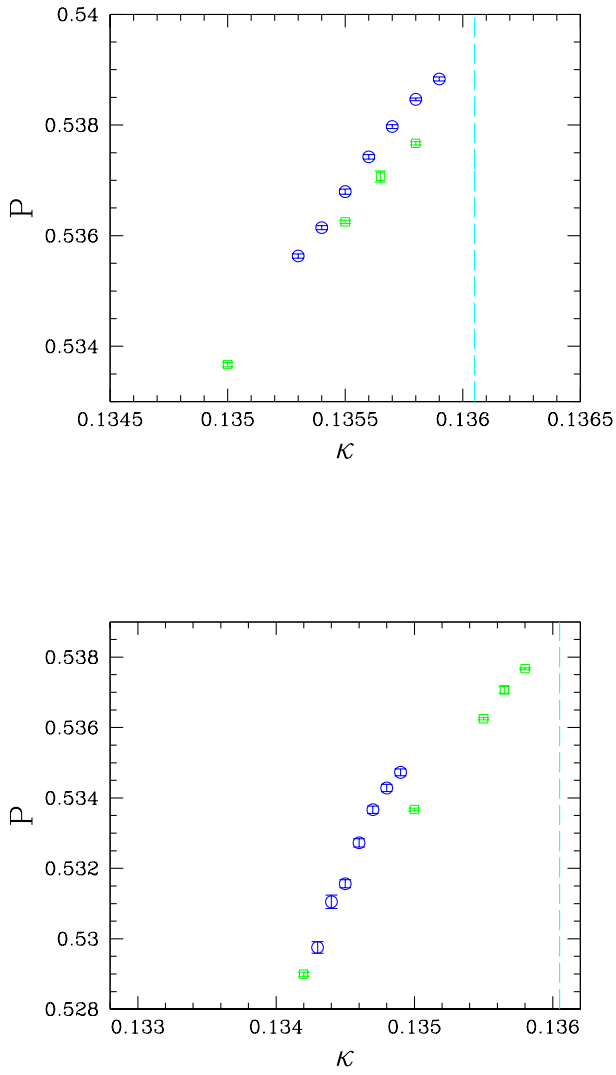

FIG. 2: The average plaquette (○) on the $24^3\,10$ (top) and $16^3\,8$ lattice (bottom) at $\beta = 5.20$, together with the average plaquette at zero temperature from the $24^3\,48$ lattice (□). The dashed line indicates the position of κ_c.

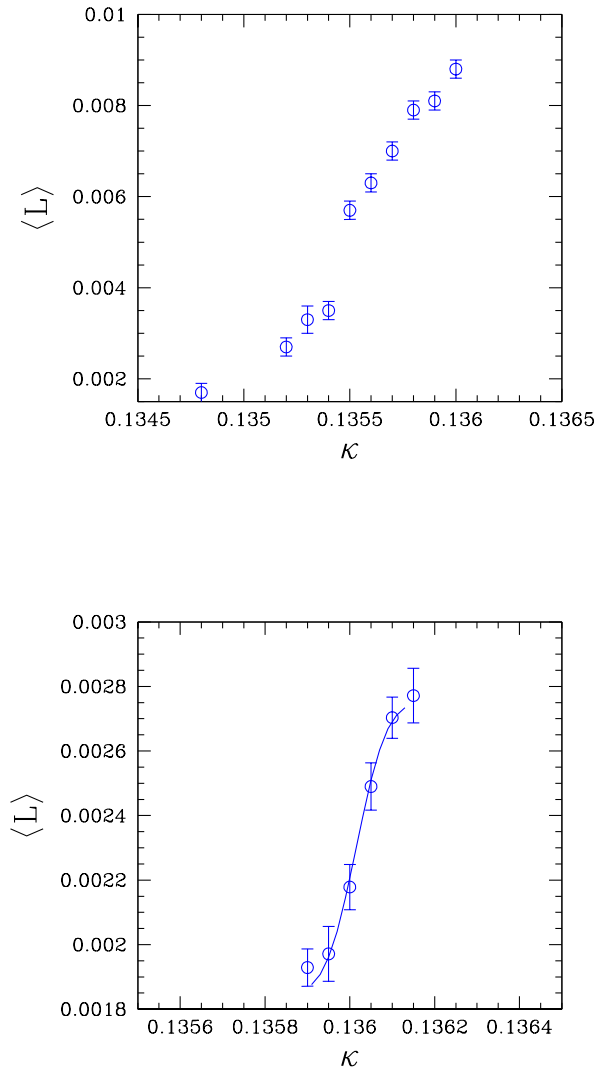

FIG. 3: The average Polyakov loop on the $24^3\,10$ (top) and $32^3\,12$ lattice (bottom) at $\beta = 5.20$ and 5.25, respectively. The solid line in the bottom figure denotes the integral of the Gaussian in Fig. 8 (bottom).

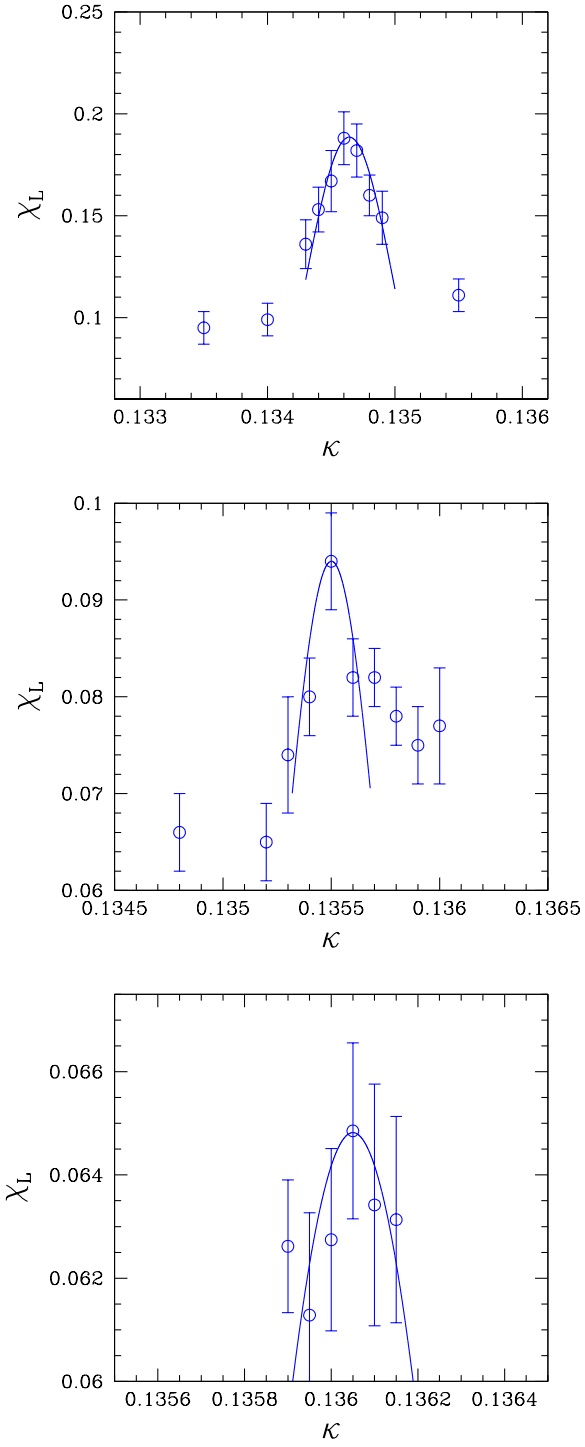

FIG. 4: The Polyakov-loop susceptibility on the $16^3\,8$ (top), $24^3\,10$ (middle) and $32^3\,12$ lattice (bottom) at $\beta = 5.20$, 5.20 and 5.25, respectively, together with a Gaussian adaptation.

and the average Polyakov loop $\langle L \rangle$, as we shall see. In Tables III–V in the Appendix we present our results for P and $\langle L \rangle$, as well as for the Polyakov-loop susceptibility χ_L. The statistical errors are computed by blocked jackknife. In Fig. 2 we plot the average plaquette P on the $24^3\,10$ and $16^3\,8$ lattice at $\beta = 5.20$. For comparison, we also show the respective numbers at zero temperature, taken from the QCDSF collaboration. Both sets of numbers agree with each other at smaller κ values (corresponding to the confined phase – see Fig. 5), as expected, while at larger κ values the finite temperature plaquette exceeds the zero temperature one, moving closer to its perturbative value. In Fig. 3 we plot the average Polyakov loop $\langle L \rangle$ on the $24^3\,10$ and $32^3\,12$ lattice at $\beta = 5.20$ and 5.25, respectively. In both cases $\langle L \rangle$ shows a sharp increase in a narrow interval of κ. Finally, in Fig. 4 we show the Polyakov-loop susceptibility for three different volumes and N_t's. While we observe a distinct peak on the $16^3\,8$ lattice, it appears that the smaller the quark mass is, the more is the peak washed out. This phenomena has also been observed by the CP-PACS group [18]. (Unfortunately, the Wuppertal group does not show the Polyakov-loop susceptibility, so we cannot compare.)

V. EQUATION OF STATE

We shall assume for the moment that the finite temperature transition of two-flavor QCD is indeed of second order in the chiral limit, as indicated in Fig. 1. Later on we shall see that our data support this view, while a first order transition appears to be unlikely. Throughout this section we shall use $\hat{\sigma}$ and $\hat{m}$ as shorthand for the subtracted chiral condensate $\langle \sigma_- \rangle$ and am, respectively.

In the vicinity of the phase transition the chiral condensate, the dynamical quark mass and the temperature are related by the equation of state

$$\hat{m} = \hat{\sigma}^\delta f(t/\hat{m}^{\frac{1}{\beta\delta}})\,, \tag{13}$$

where δ and β are the critical exponents characterizing the transition, and

$$t = \frac{T - T_c(m=0)}{T_c(m=0)} \tag{14}$$

is the reduced temperature, with $T_c(m = 0)$ being the critical temperature in the chiral limit. It is expected that the two-flavor theory is in the same universality class as the three-dimensional O(4) Heisenberg model [19], with the external magnetic field and the magnetization being identified with the bare quark mass $\hat{m}$ and the chiral condensate $\hat{\sigma}$, respectively. The critical exponents of this model were found to be [20]

$$\begin{aligned} \frac{1}{\beta\delta} &= 0.537(7)\,, \\ \frac{1}{\delta} &= 0.206(1)\,. \end{aligned} \tag{15}$$

We may expect O(4) scaling to be realized in two-flavor lattice QCD only if the fermion action obeys flavor and chiral symmetry. Neither of the common actions satisfy both. The problem of O(4) scaling has been investigated by several authors (for a review see [21]) with somewhat contradictory results. Simulations of two-flavor rooted staggered fermions [22] show deviations from O(4) scaling, albeit at small N_t. Since staggered fermions show quite large taste breaking effects at strong coupling, one might expect to find O(2) critical exponents instead. This conjecture receives support from [23]. The situation improves with the adoption of *p4* fermions. In this case evidence for O(N) scaling was found just recently [24]. For both Wilson [25] and clover fermions [26], on the other hand, it has been shown that the subtracted condensate scales with O(4) critical exponents (for $T_c(m) \geq T_c(0)$ though, see below). In [26] good agreement was found even for pion masses up to 1 GeV. At our lattice spacings, $a \approx 0.08$ fm, we find chiral symmetry to be largely restored, which manifests itself, for example, in the equality of the renormalization constants of the scalar and pseudoscalar densities, $Z_S^{Singlet} = Z_P$ [27]. So we may hope for O(4) scaling.

Let $T_c(m)$ denote the pseudocritical temperature at finite m, which we define to be the temperature corresponding to the position of the peak of the chiral susceptibility

$$\chi_\sigma = \frac{\partial\,\hat{\sigma}}{\partial\,\hat{m}}\,. \tag{16}$$

From the scaling relation (13) we then derive

$$T_c(m) - T_c(m = 0) \;\propto\; \hat{m}^{\frac{1}{\beta\delta}}\,. \tag{17}$$

Assuming

$$m_\pi^2 \propto m\,, \tag{18}$$

we thus expect to find

$$T_c(m) - T_c(m=0) \propto m_\pi^{1.07(1)} \tag{19}$$

for a second order transition at $m = 0$. A first order transition, on the other hand, would give

$$T_c(m) - T_c(m=0) \propto m_\pi^2 \,. \tag{20}$$

Alternatively, at fixed N_t, the reduced temperature t can be identified with [25]

$$t = \beta - \beta_c^{N_t} \,, \tag{21}$$

where $\beta_c^{N_t}$ is the value of β, at which the critical temperature $T_c(m)$ line hits the critical hopping parameter κ_c line as we lower β. In Fig. 5 we show the line of $T_c(m)$ in the $\kappa - \beta$ plane for $N_t = 8$, 10 and 12.

Expanding the scaling function f in (13) to lowest nontrivial order in t, *i.e.* neglecting terms of $O(t^2)$, we obtain

$$\hat{m} = A\hat{\sigma}^\delta + B\, t\, \hat{\sigma}^{\delta - \frac{1}{\beta}} \tag{22}$$

with $A, B > 0$. From (22) we can immediately read off the phase diagram in the $\kappa - \beta$ plane. This is shown in Fig. 6 for $N_t = 12$. Similar diagrams hold for different values of N_t. For

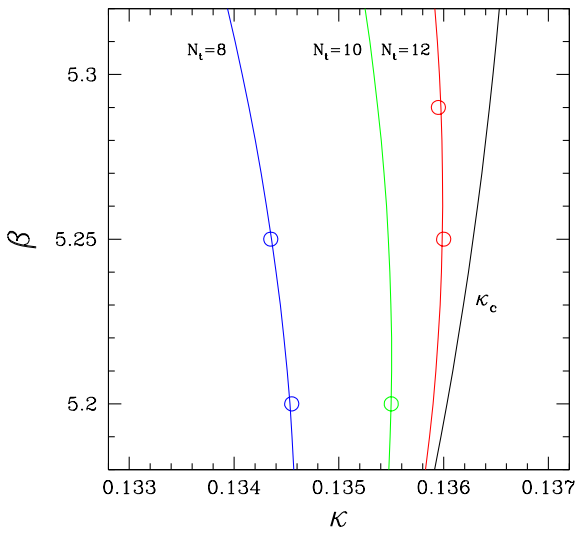

FIG. 5: The lines of critical temperature $T_c(m)$ for $N_t = 8$, 10 and 12, together with the critical hopping parameter κ_c line. The open circles refer to $T_c(m)$ obtained from the chiral susceptibility.

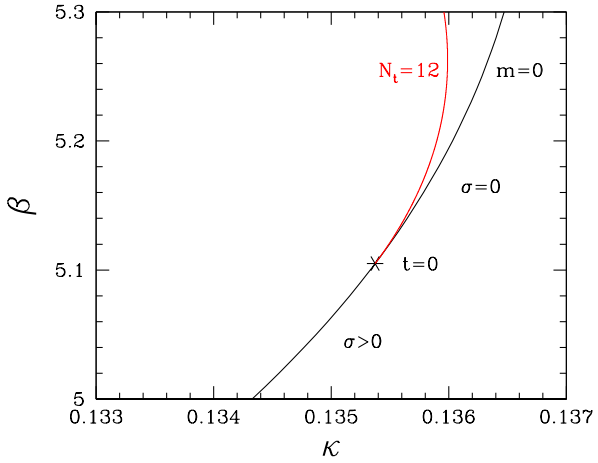

FIG. 6: The phase diagram of clover fermions for $N_t = 12$.

$t > 0$ the chiral condensate vanishes in the chiral limit. For $t < 0$, on the other hand, chiral symmetry is spontaneously broken for all κ values and

$$\hat{\sigma}^{\frac{1}{\beta}} = -\frac{B}{A}\, t \;>\; 0 \tag{23}$$

in the chiral limit. The critical temperature $T_c(m = 0)$ is obtained from N_t and the corresponding lattice spacing at $t = 0$.

VI. CHIRAL SUSCEPTIBILITY AND MAXWELL RELATION

The chiral condensate is related to the average plaquette P by means of a Maxwell relation [28]. The plaquette can be computed with high precision and so lends itself to an accurate determination of the critical temperature of the chiral transition.

Both the chiral condensate and the plaquette can be found from the partial derivatives of the partition function Z:

$$\frac{1}{V}\,\frac{\partial}{\partial\,\beta}\ln Z\bigg|_{\hat{m}} \;=\; -6\,P + 2\,\frac{\partial\,\hat{m}_c}{\partial\,\beta}\,\hat{\sigma} - 2\,\frac{\partial\,c_{SW}}{\partial\,\beta}\,\hat{\delta}\,, \tag{24}$$

$$\frac{1}{V}\,\frac{\partial}{\partial\,\hat{m}}\ln Z\bigg|_{\beta} \;=\; 2\,\hat{\sigma}\,, \tag{25}$$

where, temporarily, we have set $\hat{\sigma} = \langle\sigma\rangle$, and

$$\hat{\delta} = \langle\delta\rangle\,, \quad \delta = \frac{i}{2}\,\frac{a^3}{V}\sum_x \bar{\psi}(x)\,\sigma_{\mu\nu}\,P_{\mu\nu}(x)\,\psi(x)\,. \tag{26}$$

The second derivative $\partial^2 \ln Z / \partial\beta\, \partial\hat{m}$ can be expressed in two different orders,

$$\frac{1}{V}\frac{\partial^2}{\partial\,\beta\,\partial\,\hat{m}}\ln Z = 2\left.\frac{\partial\,\hat{\sigma}}{\partial\,\beta}\right|_{\hat{m}} = -6\left.\frac{\partial\,P}{\partial\,\hat{m}}\right|_{\beta} + 2\left.\frac{\partial\,\hat{m}_c}{\partial\,\beta}\;\frac{\partial\,\hat{\sigma}}{\partial\,\hat{m}}\right|_{\beta} - 2\left.\frac{\partial\,c_{SW}}{\partial\,\beta}\;\frac{\partial\,\hat{\delta}}{\partial\,\hat{m}}\right|_{\beta} . \tag{27}$$

Both $\hat{\sigma}$ and $\hat{\delta}$ are chiral order parameters. In the following we shall neglect the contribution from the clover term $\hat{\delta}$, mainly for the sake of clarity. We may do so, because it is suppressed by two orders of the lattice spacing with respect to the chiral condensate [29–31]:

$$\frac{\hat{\delta}}{\hat{\sigma}} = O(a^2)\,. \tag{28}$$

This leaves us with the relation

$$\left.\frac{\partial\,P}{\partial\,\hat{m}}\right|_{\beta} - \frac{1}{3}\left.\frac{\partial\,\hat{m}_c}{\partial\,\beta}\;\frac{\partial\,\hat{\sigma}}{\partial\,\hat{m}}\right|_{\beta} = -\frac{1}{3}\left.\frac{\partial\,\hat{\sigma}}{\partial\,\beta}\right|_{\hat{m}} = \frac{1}{3}\left.\frac{\partial\,\hat{m}}{\partial\,\beta}\right|_{\hat{\sigma}}\left.\frac{\partial\,\hat{\sigma}}{\partial\,\hat{m}}\right|_{\beta} . \tag{29}$$

Above identity is called the Maxwell relation. It holds for any lattice size and for all values of β and m. The right-hand form of the identity is the most useful, as it gives us the chiral susceptibility:

$$\chi_\sigma \equiv \left.\frac{\partial\,\hat{\sigma}}{\partial\,\hat{m}}\right|_{\beta} = 3\left(\frac{\partial\,\hat{m}_c}{\partial\,\beta} + \left.\frac{\partial\,\hat{m}}{\partial\,\beta}\right|_{\hat{\sigma}}\right)^{-1}\left.\frac{\partial\,P}{\partial\,\hat{m}}\right|_{\beta} = 3\left(\frac{\partial}{\partial\,\beta}\frac{1}{2\,\kappa}\right|_{\hat{\sigma}}\Bigg)^{-1}\left.\frac{\partial\,P}{\partial\,\hat{m}}\right|_{\beta} . \tag{30}$$

In both correlators, χ_σ and $(\partial\,P/\partial\,\hat{m})|_\beta$, the additive renormalization σ_0 drops out, so that we may identify $\hat{\sigma}$ with $\langle\sigma_-\rangle$ again.

Before we can identify any peak of $\partial P/\partial\hat{m}$ with a peak of χ_σ, we need to make sure that the factor in front of $\partial P/\partial\hat{m}$,

$$\mu^{-1} = 3\left(\frac{\partial\,\hat{m}_c}{\partial\,\beta} + \left.\frac{\partial\,\hat{m}}{\partial\,\beta}\right|_{\hat{\sigma}}\right)^{-1} , \tag{31}$$

is 'well behaved'. The QCDSF collaboration finds for the first term

$$\frac{\partial\,\hat{m}_c}{\partial\,\beta} = \begin{cases} -0.1536 & \beta = 5.20 \\ -0.1177 & \beta = 5.25 \\ -0.0919 & \beta = 5.29 \end{cases} . \tag{32}$$

The second term can be derived from the equation of state (22), which gives

$$\left.\frac{\partial\,\hat{m}}{\partial\,\beta}\right|_{\hat{\sigma}} = B\,\hat{\sigma}^{\delta-\frac{1}{\beta}} . \tag{33}$$

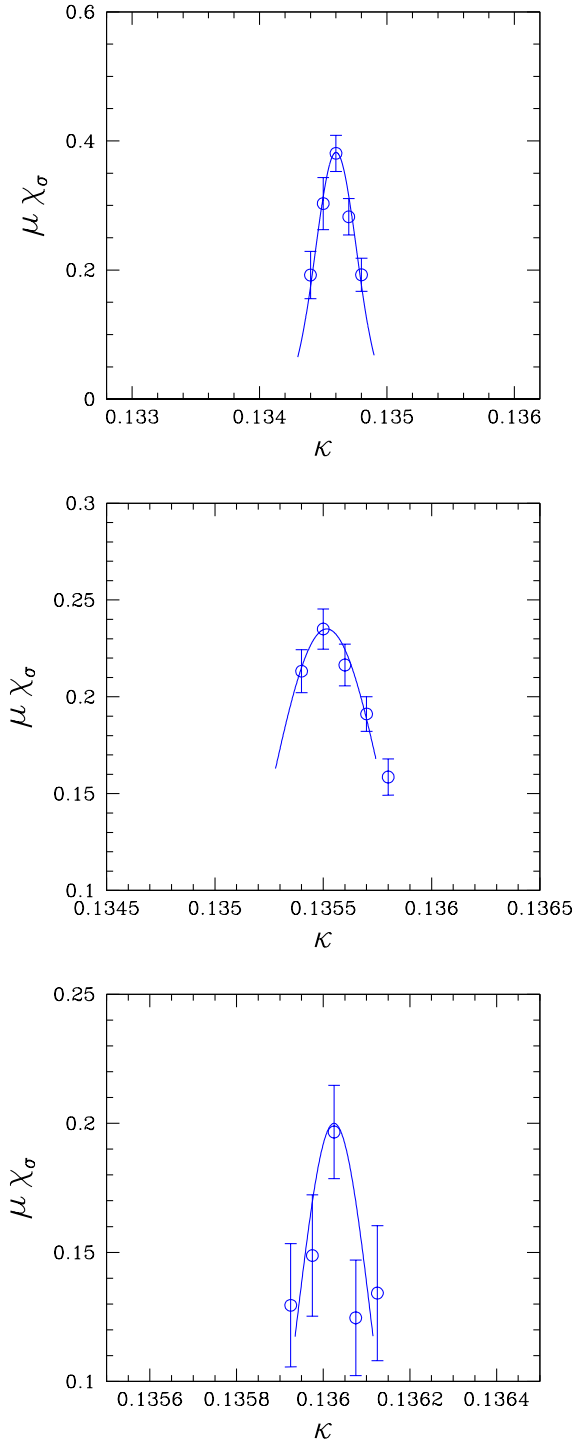

FIG. 7: The chiral susceptibility on the $16^3\,8$ (top), $24^3\,10$ (middle) and $32^3\,12$ lattice (bottom) at $\beta = 5.20$, 5.20 and 5.25, respectively, together with a Gaussian.

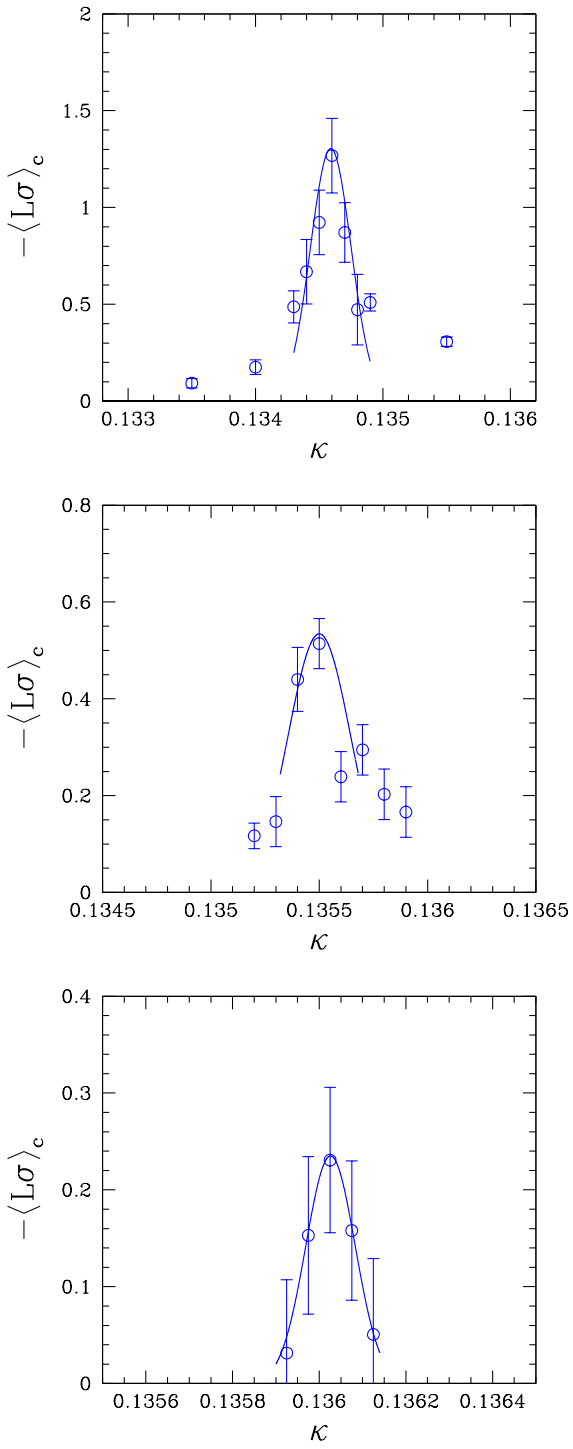

FIG. 8: The correlator $\langle L\sigma \rangle_c$ on the $16^3\,8$ (top), $24^3\,10$ (middle) and $32^3\,12$ lattice (bottom) at $\beta = 5.20$, 5.20 and 5.25, respectively, together with a Gaussian.

It vanishes proportional to $\hat{m}$ in the chiral limit, so that for small masses μ^{-1} is dominated by the first term (32).

It does not matter whether we use the renormalized or unrenormalized subtracted scalar density to determine the transition temperature, because Z_S is an extremely smooth function of $\hat{m}$ [32], which varies by less than 1% over the transition region.

The partial differential equation (29) can be solved by

$$P - P(m=0) = \frac{1}{3} \int_0^{\hat{\sigma}} d\sigma' \, \frac{\partial \, [\hat{m}_c + \hat{m}(\sigma', t)_c]}{\partial \, \beta} \,, \tag{34}$$

where we have made use of the fact that $\hat{\sigma} = 0$ in the chiral limit. For the *ansatz* (33) we find

$$P - P(m=0) = \frac{B}{3\,(\delta - \frac{1}{\beta} + 1)} \, \hat{\sigma}^{\delta - \frac{1}{\beta} + 1} + \frac{1}{3} \, \frac{\partial \, \hat{m}_c}{\partial \, \beta} \, \hat{\sigma} \,. \tag{35}$$

Knowing the critical exponents and B, we may compute the chiral condensate from the average plaquette, and *vice versa*.

The chiral transition has merely a small effect on the average plaquette. The reason is that only a fraction of a percent of the magnitude of P is of nonperturbative origin [33]. Nevertheless, with accurate data of the plaquette the Maxwell relation proves to be a viable tool to locate the position of the chiral phase transition. We use the symmetric difference quotient method,

$$f'(x) = \frac{f(x+\epsilon) - f(x-\epsilon)}{2\epsilon} \,, \tag{36}$$

to compute the derivative of the plaquette, $\partial P / \partial \hat{m}|_\beta$. In Fig. 7 we plot the chiral condensate $\mu \chi_\sigma$ as a function of κ for three representative lattices, which we chose to be the same as those in Fig. 4.

VII. TRANSITION TEMPERATURE(S)

To complete the calculation of the susceptibility $\langle \omega^2 \rangle_c$ introduced in (10), what remains to be computed is the correlator $\langle L\sigma \rangle_c$. This can be obtained from the derivative of the average Polyakov loop with respect to mass:

$$\langle L\sigma \rangle_c = \left. \frac{\partial \langle L \rangle}{\partial \hat{m}} \right|_\beta \,. \tag{37}$$

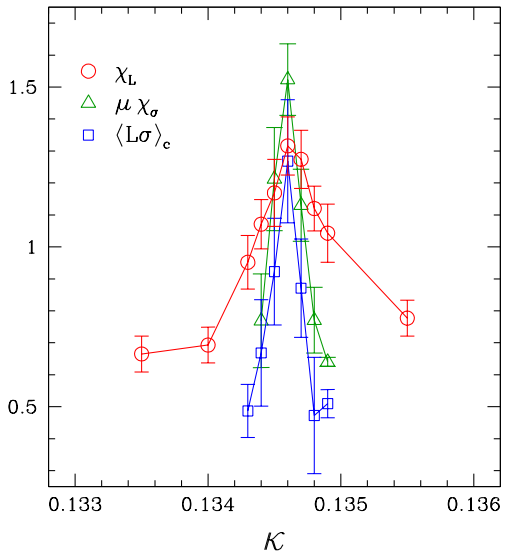

FIG. 9: The Polyakov-loop susceptibility χ_L ($\times 7$), the chiral susceptibility χ_σ ($\times 4$) and the correlator $\langle L\sigma\rangle_c$ on the $16^3\,8$ lattice at $\beta = 5.20$.

Again, the additive renormalization constant drops out in (37), and it does not make any difference whether we use the renormalized Polyakov loop [34] or not, because the renormalization factor is basically a function of β only, being an ultraviolet quantity. In Fig. 8 we plot $\langle L\sigma\rangle_c$ on the lattices of Figs. 4 and 7, where we have expressed the derivative by the symmetric difference (36) as before. Not only do we find that the Polyakov loop and the chiral condensate are strongly correlated within a narrow temperature range, but also that the position of the peaks of all three quantities, χ_L, χ_σ and $\langle L\sigma\rangle_c$, coincide within small error bars. This is illustrated once more in Fig. 9 for the $16^3\,8$ lattice at $\beta = 5.20$.

We may express the κ values by the corresponding pion masses at zero temperature. The latter are known from simulations of the QCDSF collaboration. In Table II we give the pseudocritical temperature $T_c(m)$ and the corresponding pseudocritical pion masses, $m_\pi^{T_c}$, obtained from the peak of the Polyakov-loop susceptibility, the chiral susceptibility and the correlator (37) of L and σ, respectively, and in Fig. 10 we plot the results together with an extrapolation to the chiral limit. On all lattices the individual pion masses $m_\pi^{T_c}$ are found to coincide with each other within the error bars. We do not observe any scaling violations. Our complementary runs at zero temperature did not reveal any visible scaling violations either. The spatial volume varies from $L_s(\equiv aN_s) = 1.4\,\mathrm{fm}$ to $L_s = 2.5\,\mathrm{fm}$, while the aspect

β	V	$r_0\, T_c(m)$	$r_0\, m_\pi^{T_c}$		
			χ_L	χ_σ	$\langle L\sigma\rangle_c$
5.20	$16^3\, 8$	0.682(7)	2.73(6)	2.78(6)	2.81(7)
5.20	$24^3\, 10$	0.545(6)	1.59(8)	1.59(16)	1.55(14)
5.25	$24^3\, 8$	0.735(3)	3.18(4)	3.17(4)	3.33(7)
5.25	$32^3\, 12$	0.490(2)	1.00(11)	1.05(8)	1.05(7)
5.29	$24^3\, 12$	0.517(2)	1.49(8)	1.40(9)	1.3(1)

TABLE II: The pseudocritical temperatures and corresponding pion masses obtained from the peak of χ_L, χ_σ and $\langle L\sigma\rangle_c$ on our various lattices.

ratio N_s/N_t varies between 2 and 3. Remarkably, all our results fall on a single curve. In addition, we do not see any finite size effect in direct comparison at $N_t = 8$.

The temperature $T_c(m)$ shows an almost linear behavior in the pion mass, in accord with

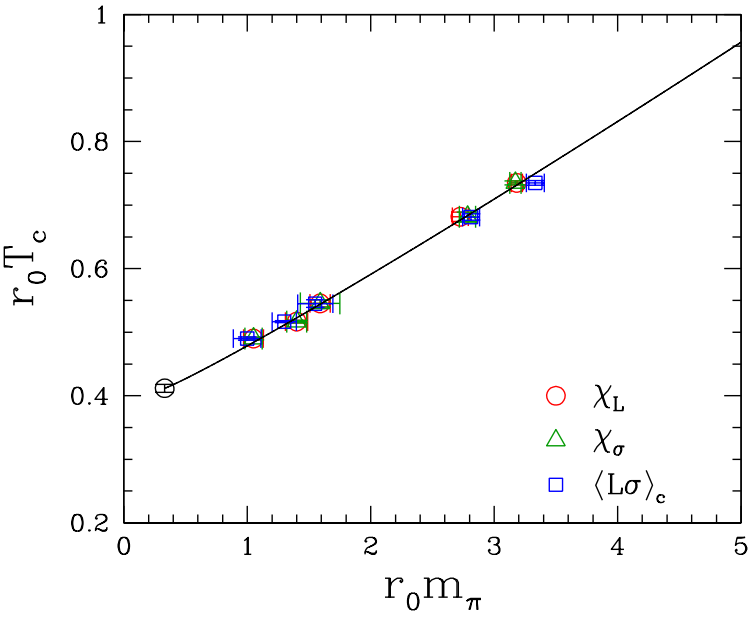

FIG. 10: The pseudocritical temperature $T_c(m)$ as a function of pion mass, together with a fit to the power $m_\pi^{1.07}$, according to the three-dimensional O(4) model.

the prediction (19) of the O(4) model. We thus may fit the data by the *ansatz*

$$T_c(m) = C + D\,(r_0\,m_\pi)^{1.07}\,. \tag{38}$$

The result is shown by the solid curve. Setting the scale by the nucleon mass, the QCDSF collaboration finds $r_0 = 0.467(15)\,\mathrm{fm}$. Using this value, we obtain at the physical pion mass

$$r_0\,T_c = 0.412(6)\,, \quad T_c = 174(3)(6)\,\mathrm{MeV}\,, \tag{39}$$

where the first error on T_c is statistical, and the second error reflects the uncertainty in setting the scale. This result is in good agreement with the deconfining transition temperature found by the Wuppertal group, but lies significantly below the result of the Brookhaven/Bielefeld collaboration.

VIII. CONCLUSIONS AND OUTLOOK

We have simulated QCD at finite temperature with two dynamical flavors of nonperturbatively improved Wilson fermions on lattices as large as $N_t = 12$ and lattice spacings as low as $0.075\,\mathrm{fm}$. The transition temperature has been computed from the Polyakov-loop susceptibility, the chiral susceptibility as well as the correlator of Polyakov loop and chiral condensate. All three temperatures are found to coincide with each other within the error bars. Our results do not support the claim of the Wuppertal group [2], albeit for $N_f = 2+1$ flavors, that the deconfining and chiral transitions take place at distinctly separated temperatures. The critical behavior appears to be in accord with the predictions of the O(4) Heisenberg model, at least as far as the quark mass dependence of T_c is concerned, while a first order transition [35] is very unlikely. However, further simulations at smaller quark masses are needed in order to confirm this conclusion beyond doubts.

The Maxwell relation has proven to be a powerful tool in unveiling the phase structure of clover fermions. It would be interesting to test (34), and the equation of state (13) itself, by direct calculation of the chiral condensate. As we already mentioned, the clover term $\hat{\delta}$ is forbidden by chiral symmetry just like $\hat{\sigma}$. So there is actually no need to neglect it (as we did) if we are just looking for a quantity which peaks at the chiral transition.

The next step is to extend the simulations to physical quark masses. Such calculations require lattices with temporal extent $N_t = 14$ and larger, given the fact that simulations

at couplings below $\beta = 5.20$ are not feasible. This requires a major increase in computing resources. Preliminary investigations at $\beta = 5.25$ indicate the existence of a transition below κ_c, resulting in $r_0 T_c(m) = 0.420(2)$. This makes us feel confident that the curve in Fig. 10 will not level off towards the staggered result [3].

Acknowledgment

We like to thank the computer centers at KEK (under the Large Scale Simulation Program No. 07-14-B), JSSC (Moscow), SC MSU (Moscow), RIKEN and HLRN (Berlin and Hannover) for their generous allocation of computer time and technical support. Furthermore, we like to thank Thomas Streuer and Hinnerk Stüben for help with the HMC code. VGB, SMM and MIP are supported in part through grants RFBR 08-02-00661, RFBR 09-02-0033, DFG-RFBR 436 RUS and NSH-679.2008.2, and like to thank their colleagues at RFNC-VNIIEF for invaluable help with the computations.

APPENDIX: TABLES OF RESULTS

$\beta = 5.20$							
$16^3\,8$				$24^3\,10$			
κ	P	$\langle L \rangle$	χ_L	κ	P	$\langle L \rangle$	χ_L
0.1330		0.0016(3)	0.075(3)	0.1348	0.467177(33)	0.0017(2)	0.066(4)
0.1335		0.0026(6)	0.095(8)	0.1352	0.464857(63)	0.0027(2)	0.065(4)
0.1340		0.0042(6)	0.099(8)	0.1353	0.464367(38)	0.0033(3)	0.074(6)
0.1343	0.469500(166)	0.0065(6)	0.136(12)	0.1354	0.463854(38)	0.0035(2)	0.080(4)
0.1344	0.468949(189)	0.0096(7)	0.153(11)	0.1355	0.463204(47)	0.0057(2)	0.094(5)
0.1345	0.468436(116)	0.0102(7)	0.167(15)	0.1356	0.462574(42)	0.0063(2)	0.082(4)
0.1346	0.467274(118)	0.0147(6)	0.188(13)	0.1357	0.462027(35)	0.0070(2)	0.082(3)
0.1347	0.466334(102)	0.0172(8)	0.182(13)	0.1358	0.461536(24)	0.0079(2)	0.078(3)
0.1348	0.465717(101)	0.0195(6)	0.160(10)	0.1359	0.461167(37)	0.0081(2)	0.075(4)
0.1349	0.465274(98)	0.0198(6)	0.149(13)	0.1360	0.460670(36)	0.0088(2)	0.077(6)
0.1355		0.0293(6)	0.111(8)				
0.1360	0.460441(57)	0.0290(4)	0.121(7)				

TABLE III: The average plaquette, the average Polyakov loop and the Polyakov-loop susceptibility on the $16^3\,8$ and $24^3\,10$ lattice at $\beta = 5.20$ against κ. The data is based on $O(10,000)$ trajectories at κ values in the immediate vicinity of the peak of the Polyakov-loop susceptibility and on $O(5,000)$ trajectories towards the edges. The numbers refer to trajectory lengths of unit one.

$\beta = 5.25$							
$16^3\,8$				$24^3\,8$			
κ	P	$\langle L\rangle$	χ_L	κ	P	$\langle L\rangle$	χ_L
0.1330	0.46879(10)	0.0025(7)	0.07(1)	0.1340	0.46326(7)	0.0090(4)	0.144(14)
0.1337		0.0057(8)	0.158(20)	0.1341	0.46258(6)	0.0127(4)	0.160(11)
0.13375	0.46454(10)	0.0065(6)	0.151(10)	0.1342	0.46197(6)	0.0148(5)	0.205(22)
0.1339	0.46370(11)	0.0084(7)	0.173(19)	0.1343	0.46151(7)	0.0164(5)	0.231(19)
0.1340	0.46315(9)	0.0105(7)	0.170(16)	0.1344	0.46080(6)	0.0188(5)	0.224(19)
0.1341	0.46267(10)	0.0115(7)	0.190(18)	0.1345	0.46030(4)	0.0205(3)	0.199(17)
0.1342	0.46188(9)	0.0145(6)	0.203(19)	0.1346	0.45985(10)	0.0220(4)	0.172(16)
0.13425	0.46152(8)	0.0167(7)	0.229(19)	$32^3\,12$			
0.1343	0.46136(8)	0.0164(5)	0.207(11)	κ	P	$\langle L\rangle$	$\langle L^2\rangle_c$
0.1344	0.46062(12)	0.0182(8)	0.200(14)	0.1359	0.45608(2)	0.00193(6)	0.0626(13)
0.1345	0.46044(26)	0.0201(7)	0.221(17)	0.13595	0.45591(3)	0.00197(8)	0.0613(20)
0.1350	0.46039(16)	0.0267(10)	0.163(17)	0.1360	0.45571(2)	0.00218(7)	0.0627(18)
0.1361	0.45479(8)	0.0328(4)	0.144(8)	0.13605	0.45544(2)	0.00249(7)	0.0649(17)
				0.1361	0.45527(2)	0.00270(6)	0.0634(23)
				0.13615	0.45509(3)	0.00277(8)	0.0631(20)

TABLE IV: The average plaquette, the average Polyakov loop and the Polyakov-loop susceptibility on the $16^3\,8$, $24^3\,8$ and $32^3\,12$ lattice at $\beta = 5.25$ against κ. The data is based on $O(10,000-15,000)$ ($O(10,000)$) trajectories at κ values in the immediate vicinity of the peak of the Polyakov-loop susceptibility and on $O(2,000-4,000)$ ($O(3,000-5,000)$) trajectories right at the edges on the $16^3\,8$ ($24^3\,8$) lattice. On the $32^3\,12$ lattice we have accumulated $O(3,000-7,000)$ trajectories at the individual κ values.

$\beta = 5.29 \quad 24^3\,12$			
κ	P	$\langle L \rangle$	χ_L
0.1357	0.45223(4)	0.00165(15)	0.0665(38)
0.1358	0.45185(2)	0.00184(10)	0.0667(18)
0.1359	0.45153(2)	0.00238(11)	0.0695(21)
0.1360	0.45114(3)	0.00272(11)	0.0684(19)
0.1361	0.45086(4)	0.00340(11)	0.0623(27)

TABLE V: The average plaquette, the average Polyakov loop and the Polyakov-loop susceptibility on the $24^3\,12$ lattice at $\beta = 5.29$ against κ. The data is based on $O(5,000)$ trajectories at the central κ values and on $O(2,000 - 3,000)$ trajectories at the outer κ values.

[1] M. Cheng, N. H. Christ, S. Datta, J. van der Heide, C. Jung, F. Karsch, O. Kaczmarek, E. Laermann, R. D. Mawhinney, C. Miao, P. Petreczky, K. Petrov, C. Schmidt and T. Umeda, Phys. Rev. D **74**, 054507 (2006) [arXiv:hep-lat/0608013].

[2] Y. Aoki, Z. Fodor, S. D. Katz and K. K. Szabo, Phys. Lett. B **643**, 46 (2006) [arXiv:hep-lat/0609068].

[3] M. Cheng, N. H. Christ, S. Datta, J. van der Heide, C. Jung, F. Karsch, O. Kaczmarek, E. Laermann, R. D. Mawhinney, C. Miao, P. Petreczky, K. Petrov, C. Schmidt, W. Soeldner and T. Umeda, Phys. Rev. D **77**, 014511 (2008) [arXiv:0710.0354 [hep-lat]].

[4] Y. Aoki, S. Borsanyi, S. Dürr, Z. Fodor, S. D. Katz, S. Krieg and K. K. Szabo, JHEP **0906**, 088 (2009) [arXiv:0903.4155 [hep-lat]].

[5] A. Bazavov, T. Bhattacharya, M. Cheng, N. H. Christ, C. DeTar, S. Ejiri, S. Gottlieb, R. Gupta, U. M. Heller, K. Huebner, C. Jung, F. Karsch, E. Laermann, L. Levkova, C. Miao, R. D. Mawhinney, P. Petreczky, C. Schmidt, R. A. Soltz, W. Soeldner, R. Sugar, D. Toussaint and P. Vranas, Phys. Rev. D **80**, 014504 (2009) [arXiv:0903.4379 [hep-lat]].

[6] S. Roessner, T. Hell, C. Ratti and W. Weise, Nucl. Phys. A **814**, 118 (2008) [arXiv:0712.3152 [hep-ph]].

[7] S. Digal, E. Laermann and H. Satz, Eur. Phys. J. C **18**, 583 (2001) [arXiv:hep-ph/0007175].

[8] S. Digal, E. Laermann and H. Satz, Nucl. Phys. A **702**, 159 (2002).

[9] K. Fukushima, Phys. Lett. B **553**, 38 (2003) [arXiv:hep-ph/0209311].

[10] K. Fukushima, Phys. Rev. D **68**, 045004 (2003) [arXiv:hep-ph/0303225].

[11] V. G. Bornyakov, S. M. Morozov, Y. Nakamura, M. I. Polikarpov, G. Schierholz and T. Suzuki, PoS **LAT2007**, 171 (2007) [arXiv:0711.1427 [hep-lat]].

[12] K. Jansen and R. Sommer, Nucl. Phys. B **530**, 185 (1998) [Erratum-ibid. B **643**, 517 (2002)] [arXiv:hep-lat/9803017].

[13] A. Ali Khan, T. Bakeyev, M. Göckeler, R. Horsley, D. Pleiter, P. Rakow, A. Schäfer, G. Schierholz and H. Stüben, Phys. Lett. B **564**, 235 (2003) [arXiv:hep-lat/0303026]; A. Ali Khan, T. Bakeyev, M. Göckeler, R. Horsley, D. Pleiter, P. E. L. Rakow, A. Schäfer, G. Schierholz and H. Stüben, Nucl. Phys. Proc. Suppl. **129**, 853 (2004) [arXiv:hep-lat/0309078].

[14] M. Hasenbusch, Phys. Lett. B **519**, 177 (2001) [arXiv:hep-lat/0107019].

[15] J. C. Sexton and D. H. Weingarten, Nucl. Phys. B **380**, 665 (1992).

[16] M. Göckeler, R. Horsley, Y. Nakamura, H. Perlt, D. Pleiter, P. E. L. Rakow, G. Schierholz, A. Schiller, T. Streuer, H. Stüben and J. M. Zanotti, PoS **LAT2007**, 041 (2007) [arXiv:0712.3525 [hep-lat]]; N. Cundy, M. Göckeler, R. Horsley, T. Kaltenbrunner, A. D. Kennedy, Y. Nakamura, H. Perlt, D. Pleiter, P. E. L. Rakow, A. Schäfer, G. Schierholz, A. Schiller, H. Stüben and J. M. Zanotti, Phys. Rev. D **79**, 094507 (2009) [arXiv:0901.3302 [hep-lat]].

[17] A. Ali Khan, T. Bakeyev, M. Göckeler, T. R. Hemmert, R. Horsley, A. C. Irving, B. Joó, D. Pleiter, P. E. L. Rakow, G. Schierholz and H. Stüben, Nucl. Phys. B **689**, 175 (2004) [arXiv:hep-lat/0312030]; M. Göckeler, R. Horsley, A. C. Irving, D. Pleiter, P. E. L. Rakow, G. Schierholz and H. Stüben, Phys. Lett. B **639**, 307 (2006) [arXiv:hep-ph/0409312]; M. Göckeler, R. Horsley, A. C. Irving, D. Pleiter, P. E. L. Rakow, G. Schierholz and H. Stüben, Phys. Rev. D **73**, 014513 (2006) [arXiv:hep-ph/0502212]; M. Göckeler, R. Horsley, A. C. Irving, D. Pleiter, P. E. L. Rakow, G. Schierholz, H. Stüben and J. M. Zanotti, Phys. Rev. D **73**, 054508 (2006) [arXiv:hep-lat/0601004].

[18] A. Ali Khan, S. Aoki, R. Burkhalter, S. Ejiri, M. Fukugita, S. Hashimoto, N. Ishizuka, Y. Iwasaki, K. Kanaya, T. Kaneko, Y. Kuramashi, T. Manke, K.-I. Nagai, M. Okamoto, M. Okawa, H. P. Shanahan, Y. Taniguchi, A. Ukawa and T. Yoshié, Phys. Rev. D **64**, 074510 (2001) [arXiv:hep-lat/0103028].

[19] R. D. Pisarski and F. Wilczek, Phys. Rev. D **29**, 338 (1984).

[20] K. Kanaya and S. Kaya, Phys. Rev. D **51**, 2404 (1995) [arXiv:hep-lat/9409001]; P. Butera and M. Comi, Phys. Rev. B **52**, 6185 (1995) [arXiv:hep-lat/9505027]; H. G. Ballesteros, L. A. Fernandez, V. Martin-Mayor and A. Munoz Sudupe, Phys. Lett. B **387**, 125 (1996) [arXiv:cond-mat/9606203].

[21] C. DeTar and U. M. Heller, Eur. Phys. J. A **41**, 405 (2009) [arXiv:0905.2949 [hep-lat]].

[22] T. Mendes, PoS **LAT2007**, 208 (2007) [arXiv:0710.0746 [hep-lat]].

[23] J. B. Kogut and D. K. Sinclair, Phys. Rev. D **73**, 074512 (2006) [arXiv:hep-lat/0603021].

[24] S. Ejiri *et al.*, Phys. Rev. D **80**, 094505 (2009) [arXiv:0909.5122 [hep-lat]].

[25] Y. Iwasaki, K. Kanaya, S. Kaya and T. Yoshié, Phys. Rev. Lett. **78**, 179 (1997) [arXiv:hep-lat/9609022].

[26] A. Ali Khan, S. Aoki, R. Burkhalter, S. Ejiri, M. Fukugita, S. Hashimoto, N. Ishizuka, Y. Iwasaki, K. Kanaya, T. Kaneko, Y. Kuramashi, T. Manke, K. Nagai, M. Okamoto, M. Okawa, A. Ukawa, T. Yoshié, Phys. Rev. D **63**, 034502 (2001) [arXiv:hep-lat/0008011].

[27] QCDSF collaboration, work in progress.

[28] M. Göckeler, R. Horsley, V. Linke, P. E. L. Rakow, G. Schierholz and H. Stüben, Nucl. Phys. B **487**, 313 (1997) [arXiv:hep-lat/9605035].

[29] M. Kremer and G. Schierholz, Phys. Lett. B **194**, 283 (1987).

[30] T. Doi, N. Ishii, M. Oka and H. Suganuma, Prog. Theor. Phys. Suppl. **151**, 161 (2003) [arXiv:hep-lat/0303014].

[31] A. Di Giacomo and Yu. A. Simonov, Phys. Lett. B **595**, 368 (2004) [arXiv:hep-ph/0404044].

[32] M. Göckeler, R. Horsley, A. C. Irving, D. Pleiter, P. E. L. Rakow, G. Schierholz and H. Stüben, Phys. Lett. B **639**, 307 (2006) [arXiv:hep-ph/0409312].

[33] R. Horsley, P. E. L. Rakow and G. Schierholz, Nucl. Phys. Proc. Suppl. **106**, 870 (2002) [arXiv:hep-lat/0110210].

[34] O. Kaczmarek, F. Karsch, P. Petreczky and F. Zantow, Phys. Lett. B **543**, 41 (2002) [arXiv:hep-lat/0207002].

[35] G. Cossu, M. D'Elia, A. Di Giacomo and C. Pica, PoS **LAT2007**, 219 (2007) [arXiv:0710.0174 [hep-lat]].